RSC Advances

Cite this: *RSC Advances*, 2012, **2**, 6011–6017

www.rsc.org/advances

**PAPER**

# Photo-induced electron transfer study of D-π-A sensitizers with different type of anchoring groups for dye-sensitized solar cells†

**Yan Hao,[a] Xichuan Yang,*[a] Jiayan Cong,[a] Xiao Jiang,[a] Anders Hagfeldt[b] and Licheng Sun*[ac]**

***Received 9th March 2012, Accepted 21st April 2012***
**DOI: 10.1039/c2ra20436c**



A new D-π-A organic dye **HY102** with a lateral anchoring group and two reference dyes **HY102-1** (using cyanoacrylic acid as an electron acceptor and the anchoring group) and **HY102-2** (containing both cyanoacrylic acid and lateral carboxylic acid) have been synthesized. The optical and electrochemical test results from the three different styles of photosensitizers show that the excited electrons of the novel dye **HY102** with lateral carboxylic acid group most probably are injected into the CB of $TiO_2$ through the electron acceptor moiety close to the $TiO_2$ surface by spatial transfer, not through the lateral anchoring group of the carboxylic acid. Research into the photo-induced electron transfer of the novel sensitizers with lateral anchoring system is reasonable and crucial for further improving efficiencies by modifying the molecular structures.

## Introduction

With increasing concerns about the energy crisis and accompanying environmental issues, the development of clean and sustainable energy technologies has been a subject of intense research to scientists. Dye-sensitized Solar Cells (DSCs) featuring low cost and easy fabrication when compared to the ubiquitous silicon solar cells have exhibited the highest efficiency up to 12% under laboratory conditions.[1] D-π-A constructed organic dyes are known for their excellent high extinction molar coefficients, easy design and optimization of molecular structures, and simple preparation, making them attractive for DSCs.[2] However, most of D-π-A organic dyes have a cyanoacrylic acid as the anchoring group. This has limited the fine-tuning of HOMO-LUMO levels due to the difficulty in changing the structure of the anchoring group and the electron acceptor part. With above consideration, previously, a new strategy to design organic dyes for DSCs has been developed, in which the anchoring group is separated from the electron acceptor groups of the dyes.[3] The excited electrons in the new style of dyes are expected to be injected into the conduction band (CB) of $TiO_2$ through the electron acceptor moiety rather than the anchoring group. However, the efficiency of this kind of dye is still lower than that of the state of the art organic dyes. In order to further investigate the effect of the lateral anchoring group on the performance of DSCs, a photo-induced electron transfer study of D-π-A sensitizers with a lateral anchoring group and a normal cyanoacrylic acid anchoring group is studied in this paper.

The traditional cyanoacrylic acid definitely plays a crucial role in $TiO_2$ sensitization and electron injection and many studies have been performed to investigate the electron transfer process between the electron acceptor unit and the semiconductor.[4,5] But, the electron injection process of the novel sensitizers with lateral anchoring groups is still under discussion. Therefore, to obtain a clearer understanding, we have studied the optical and electrochemical properties of lateral dyes compared with cyanoacrylic acid dyes. A new D-π-A organic dye **HY102** with the lateral anchoring group and two reference of dyes **HY102-1** using cyanoacrylic acid as electron acceptor and the anchoring group and **HY102-2** containing both cyanoacrylic acid and lateral carboxylic acid were synthesized (Fig. 1). The results show that **HY102** displays an obvious change in optical and redox properties due to the introduction of the stronger electron withdrawing unit, which plays a beneficial role on the

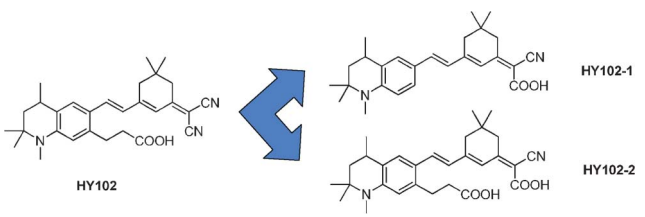


**Fig. 1** Molecular structures of **HY102**, **HY102-1** and **HY102-2**.

[a]*State Key Laboratory of Fine Chemicals, DUT-KTH Joint Education and Research Centre on Molecular Devices, Dalian University of Technology (DUT), 2 Linggong Rd, 116024, Dalian, China. E-mail: yangxc@dlut.edu.cn.; Fax: +86 411 84986250; Tel: +86 411 84986247*
[b]*Department of Physical and Analytical Chemistry, Uppsala University, Box 259 SE-751 05, Uppsala, Sweden*
[c]*School of Chemical Science and Engineering, Department of Chemistry, KTH Royal Institute of Technology, Teknikringen, 30, 10044, Stockholm, Sweden. E-mail: lichengs@kth.se.; Fax: +46 8 791 2333; Tel: +46 8 790 8127*

† Electronic Supplementary Information (ESI) available: Details of the synthesis and characterization of HY102, HY102-1 and HY102-2, procedures of fabricating the DSCs, materials and methods of measurements and calculations. See DOI: 10.1039/c2ra20436c

light-harvesting properties of the dyes compared to two other reference dyes. It is concluded therefore that D-π-A organic near-infrared dyes can be achieved by introducing a lateral anchoring group into the dye framework. It is noteworthy that, according to our research, the novel lateral dye **HY102** presents a poor photovoltaic performance, which is attributed to poor injection of excited electrons into the CB of $TiO_2$ through the electron acceptor moiety being spatially close to the $TiO_2$ surface, and not from the anchoring group more commonly observed in sensitizers with cyanoacrylic acid as an end-group, such as **HY102-1** and **HY102-2**.

## Results and discussion

### Synthesis

Tetrahydroquinoline derivatives **1–5** and **D1** (Scheme 1) were synthesized in our previous publication.[3] Scheme 2 shows the synthetic routes of compounds **6–8** and **D2** according to the already reported procedures.[6] Intermediates **9** and **A2** were prepared following the reported procedure.[7] Finally, the Knoevenagel condensation reactions were performed to get compounds **9** and **A2** through the aldehydes **D1** and **D2** compounds respectively then the hydrolysis reaction gave the target dyes **HY102**, **HY102-1** and **HY102-2** (Scheme 3). The detailed synthetic procedures are described in the Supporting Information†.

### Photophysical properties

Absorption spectra of the dyes **HY102**, **HY102-1** and **HY102-2** in $CH_2Cl_2$ solutions are shown in Fig. 2. The characteristic data are collected in Table 1. Three compounds **HY102**, **HY102-1** and **HY102-2** all exhibit a broad absorption band in the visible region, appearing at 533 nm, 514 nm and 485 nm, respectively. Compared with **HY102-1**, the maximum absorption of **HY102** was red-shifted by 19 nm because of the introduction of the stronger electron withdrawing group (2-methylenemalononitrile) as the acceptor part. It can be concluded that the novel D-π-A organic dyes with the lateral anchoring group are more prone to adjust the absorption spectra into the near infrared region than conventional D-π-A organic dyes by modifying the electron acceptor and anchoring part. Generally, this red shift is

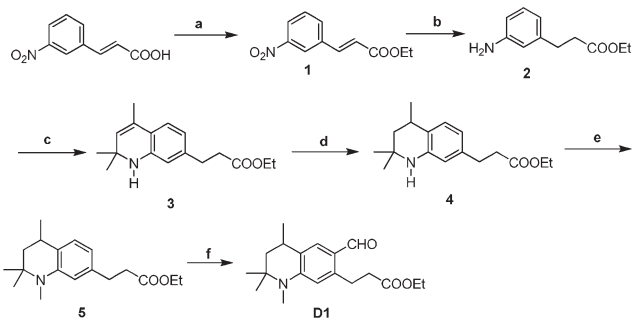


**Scheme 1** Synthetic routes of mediates 1-**D1**. Reagents and conditions: (a) EtOH, concentrated $H_2SO_4$, reflux overnight, 95%; (b) EtOH, Pd/C (5%), 4 h, 89%; (c) acetone, *p*-TsOH, cyclohexane, 80–90 °C, 8–10 h, 22%; (d) Raney-Ni, $H_2$, 1 MPa, 130 °C, 99%; (e) $(CH_3)_2SO_4$, benzene, reflux overnight, 68%; (f) DMF/$POCl_3$, 55 °C, 6 h, 76%.

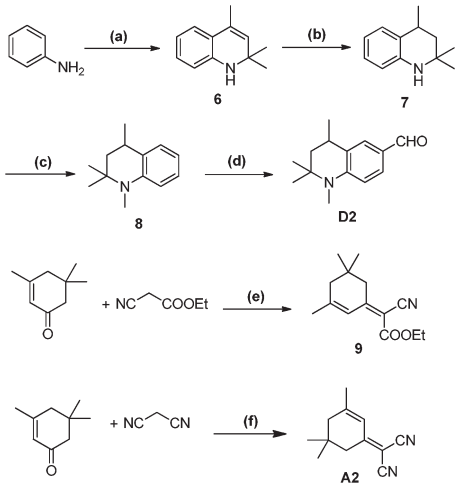


**Scheme 2** Synthetic routes of compounds 6-**D2**, 9 and **A2**. Reagents and conditions: (a) acetone, *p*-TsOH, cyclohexane, 80–90 °C, 8–10 h; (b) Raney-Ni, $H_2$, 1 MPa, 130 °C; (c) $(CH_3)_2SO_4$, benzene, reflux overnight; (d) DMF/$POCl_3$, 55 °C, 6 h, 76%. (e)$CH_3COONH_4$, $CH_3COOH$; (f)$CH_3CN$, piperidine.

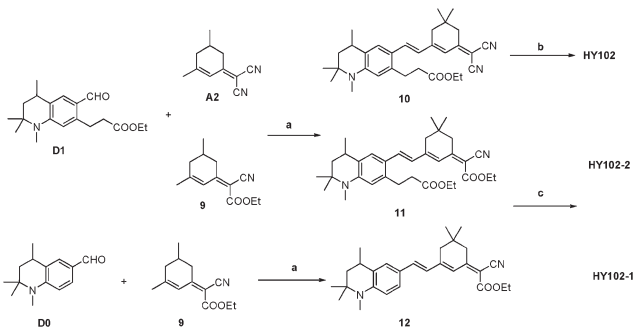


**Scheme 3** Synthetic routes of dyes **HY102**, **HY102-1** and **HY102-2**. Reagents and conditions: (a) $CH_3CN$, piperidine, reflux, over night; (b) $CH_3CH_2OH$, LiOH/$H_2O$, room temperature; (c) $CH_3CH_2OH$, LiOH/$H_2O$, 50 °C, 1 h.

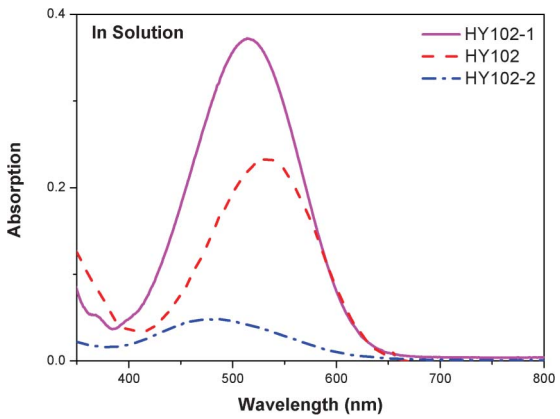


**Fig. 2** UV-vis spectra of dyes **HY102**, **HY102-1** and **HY102-2** ($2 \times 10^{-5}$ M) in $CH_2Cl_2$.

anticipated to increase the photocurrent of DSCs. However, the sensitizer **HY102-2**, which has an additional lateral part than **HY102-1**, has dramatically blue shifted the absorption spectrum and given a remarkably decreased molar extinction coefficient,

 

**Table 1** Absorption and electrochemical properties of **HY102**, **HY102-1** and **HY102-2**

| Dye | Absorption | | | | | |
|---|---|---|---|---|---|---|
| | $\lambda_{max}$ [a] (nm) | $\varepsilon(M^{-1}cm^{-1})$ | $\lambda_{max}$ on $TiO_2$ [b] (nm) | $E_{0\text{-}0}$ [d] (eV) | $E_{ox}$ [c] (V) | $E_{ox}$-$E_{0\text{-}0}$ (V) |
| **HY102** | 533 | 11 719 | 540 | 1.83 | 0.83 | −1.00 |
| **HY102-1** | 514 | 18 620 | 536 | 1.85 | 0.82 | −1.03 |
| **HY102-2** | 485 | 2415 | 502 | 1.90 | 0.77 | −1.13 |

[a] Absorption spectra were measured in $CH_2Cl_2$ solution at room temperature. [b] Absorption spectra on $TiO_2$ were obtained through measuring the dye adsorbed on $TiO_2$ film in $CH_2Cl_2$. [c] The oxidation potential of the dyes were measured in $CH_2Cl_2$ with 0.1 M tetrabutylammonium hexafluorophosphate ($TBAPF_6$) as electrolyte (working electrode: glassy carbon; reference electrode: $Ag/Ag^+$; calibrated with ferrocene/ferrocenium ($Fc/Fc^+$) as an internal reference and converted to NHE by addition of 440 mV, counter electrode: Pt). [d] $E_{0\text{-}0}$ was estimated from onset point of absorption spectra on $TiO_2$ film.

only 2415 $M^{-1}$ $cm^{-1}$ at 485 nm. The poor light harvesting ability of HY**102-2** may be caused by the decrease of coplanarity between the electron donor and the electron acceptor in the ground-state as well as in the excited-state due to the existence of two carboxyl acid groups.

From the absorption spectra of **HY102**, **HY102-1** and **HY102-2** on the $TiO_2$ surface, the maximum absorptions were all red-shifted compared to that in solution, 7 nm, 22 nm and 17 nm, respectively, as shown in Fig. 3. The red shifts of spectra for these dyes could be caused by well-known solvent effects. In addition, the tendency to *J*-aggregation of dye molecules onto the $TiO_2$ surface may also contribute to this red shift.[8] Obviously, the absorption region of **HY102**, **HY102-1** and **HY102-2** on $TiO_2$ are broader than that those in solution, from 400 nm–700 nm, which is an advantageous spectral property for light harvesting of the solar spectrum. This result indicates that bathochromically shifted absorption spectra for all three dyes on the $TiO_2$ surface were favorable for light harvesting and high photocurrent.

### Electrochemical properties

The electrochemical properties of sensitizers **HY102**, **HY102-1** and **HY102-2** were investigated in $CH_2Cl_2$ containing 0.1 M $TBAPF_6$ as the electrolyte at room temperature. The electrochemical data are summarized in Table 1. The oxidation potentials ($E_{ox}$) corresponding to the HOMO levels of the dyes can be obtained by cyclic voltammetry measurements, the excited state oxidation potential ($E_{ox}$*) corresponding to the LUMO levels of the dyes were calculated by $E_{ox} - E_{0\text{-}0}$, where $E_{0\text{-}0}$ is the zero-zero energy of the dyes estimated from the onset point of absorption spectra on $TiO_2$. In these dyes, the novel lateral sensitizer **HY102** with a stronger electron withdrawing unit (2-methylenemalononitrile) instead of cyanoacrylic acid as the electron acceptor shows positive shifts at both HOMO and LUMO levels compared to the reference dyes. Furthermore, the relatively strong influence of the stronger electron acceptor on the LUMO level of **HY102** makes the $E_{0\text{-}0}$ value decrease, and consequently results in a red shift of the absorption spectrum. As shown in Table 1, the excited state oxidation potentials of all these dyes are much more negative than the conduction band edge of $TiO_2$, which is located at *ca.* −0.5 V (*vs* NHE), and the ground state oxidation potentials of these dyes, are more positive than the iodine redox potential value (+0.4 V *vs* NHE). As a result, a sufficient thermodynamic driving force for the efficient electron injection to $TiO_2$ film and the dye regeneration reaction from iodine redox couple can be provided.[9]

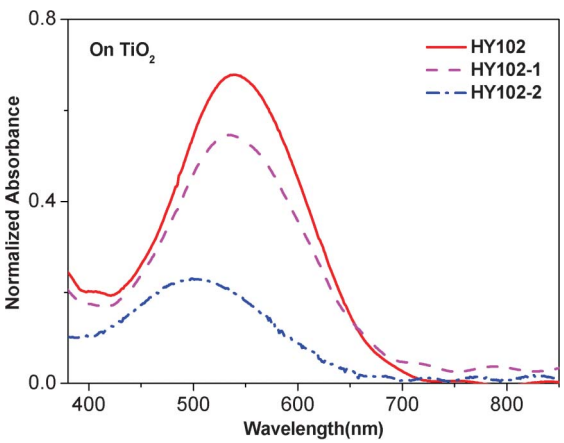


**Fig. 3** UV-vis spectra of dyes **HY102**, **HY102-1** and **HY102-2** on $TiO_2$ film.

To gain the further insight into the molecular structure and electron distribution of these three dyes at the frontier and nearby molecular orbitals, we performed quantum-chemical calculations on the dyes **HY102**, **HY102-1** and **HY102-2** using DFT calculations with the Gaussian 03 program. The calculations were carried out with B3LYP under 6-31+G(d) basis set, given the negligible effect of salvation on the electronic structure. The molecular structure and electron distributions of the HOMO and LUMO levels of three dyes are shown in Fig. 4. We observed that HOMO-LUMO excitation induced by light irradiation could move the electron distribution from the whole molecule to the cyanoacrylic acid moieties for **HY102-1**. For the dyes **HY102** and **HY102-2** containing the lateral carboxylic acid, the electron distributions were located totally at the electron acceptor part, nothing at the lateral anchoring unit. The reason for this phenomenon may be due mainly to the flexible lateral carboxylic acid group incorporated into the framework by single bonds, which cannot participate in the $\pi$-conjugated system and attract electrons. As a result, according to theoretical calculations, providing a similar molecular orbital geometry when anchored to $TiO_2$, the excited electron for the lateral dye **HY102** on $TiO_2$ should be injected into the conduction band of $TiO_2$ mainly through the acceptor part, not the lateral carboxylic acid.

### Photovoltaic performance

The dye-sensitized solar cells were constructed by using the three dyes as a sensitizer and nanocrystalline anatase $TiO_2$ as the semiconductor material. The device performance parameters

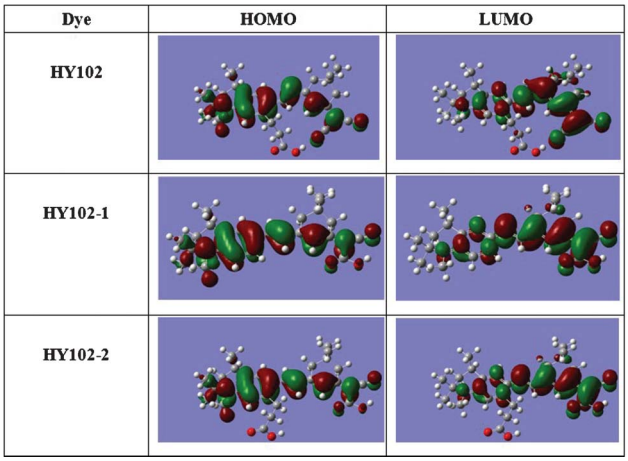


**Fig. 4** Calculated isodensity surface plots and molecular orbital energy diagram of the HOMO and LUMO for **HY102**, **HY102-1** and **HY102-2**.

under AM 1.5 illumination are collected in Table 2. Fig. 5 and Fig. 7 show the photocurrent-voltage (*J-V*) curves and the incident photon-to-current conversion efficiencies (IPCE) of selected cells, respectively. The optimized evaluation conditions are determined to be $2 \times 10^{-4}$ M of dye in $CH_2Cl_2$ solution, $2 \times 10^{-4}$ M chenodeoxycholic acid (CDCA) as a coadsorbent, and the electrolyte is 0.6 M 1,2-dimethyl-3-*n*-propylimidazolium iodide (DMPII)/0.06 M LiI/0.04 M $I_2$/0.4 M 4-*tert*-butylpyridine(TBP) in acetonitrile for **HY102-1**. Noticeably, the optimized test condition for **HY102** and **HY102-2** were different from **HY102-1**, which were determined to be $2 \times 10^{-4}$ M of dye in $CH_2Cl_2$ solution and the electrolyte is 0.6 M DMPII/0.5 M LiI/0.02 M $I_2$/0.1 M tetrabutyl ammonium iodide (TBAI) in acetonitrile : valeronitrile (AN : VN) = 85 : 15. Under the optimized test condition, the **HY102-1**-sensitized solar cell showed the best efficiency at 7.0% of all three dyes, with a $J_{sc}$ of 13.96 mA $cm^{-2}$, a $V_{oc}$ of 0.710 V, and an *FF* of 0.71. However, the lateral dye **HY102**-sensitized solar cell rendered an efficiency of 2.7% with $J_{sc}$ of 7.55 mA $cm^{-2}$, $V_{oc}$ of 0.54 V, and *FF* of 0.66. The photovoltaic performance is evidently decreased in the lateral dye **HY102** compared with **HY102-1** as a result of the poor electron injection efficiency from the excited dye to the conduction band of $TiO_2$. Such a result was further investigated and discussed through the study of the mechanism of the electron injection to the conduction band of $TiO_2$ for the DSCs based on the novel lateral sensitizer **HY102** relative to **HY102-1** and **HY102-2**.

Coadsorbent of CDCA is often utilized to suppress the dye aggregation by coadsorption with sensitizer on TiO2 surface,

**Table 2** Photovoltaic performance of DSCs based on **HY102**, **HY102-1** and **HY102-2** dyes[a]

| Dyes | Solvents | $J_{sc}$ (mA/cm$^2$) | $V_{oc}$ (mV) | *FF* | $\eta$ (%) |
|---|---|---|---|---|---|
| **HY102** | $CH_2Cl_2$ | 7.55 | 540 | 0.66 | 2.7 |
| **HY102-1** | $CH_2Cl_2$ | 13.96 | 710 | 0.71 | 7.0 |
| **HY102-2** | $CH_2Cl_2$ | 10.80 | 581 | 0.57 | 3.6 |

[a] Irradiated light: AM 1.5 G (100 mW $cm^{-2}$); Working area: 0.159 $cm^2$; Electrolyte: 0.6 M DMPII, 0.06 M LiI, 0.04 M $I_2$, 0.4 M TBP in acetonitrile for **HY102-1** and 0.6 M DMPII/0.5 M LiI/0.02 M $I_2$/0.1 M TBAI in AN:VN = 85:15 for **HY102** and **HY102-2**.

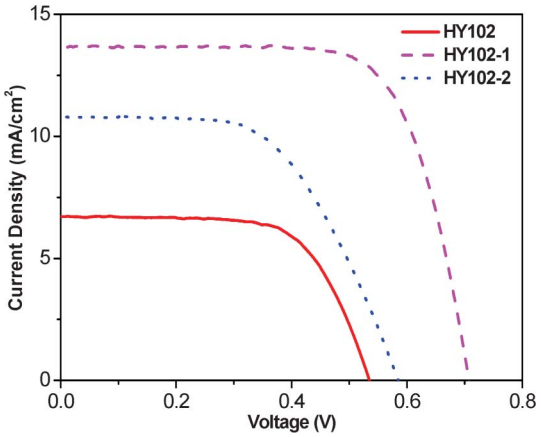


**Fig. 5** *J-V* curves of DSCs based on **HY102**, **HY102-1** and **HY102-2** dyes under optimized work conditions.

thus improving the photovoltaic performance.[10] It has been reported[11] that tetrahydroquinoline dyes easily aggregate on $TiO_2$ film. Therefore, CDCA was added into the three dye solution and expected to give a better DSC performance. The sensitized results show that only the conventional dye **HY102-1** could be adsorbed on the $TiO_2$ surface perfectly with CDCA. But the lateral dyes **HY102** and **HY102-2** cannot be loaded onto $TiO_2$ film in the presence of CDCA. This result implies that CDCA has much stronger competitive adsorption ability on the $TiO_2$ surface than the lateral sensitizers. It is suggested that the sensitizers with lateral anchoring group adsorb to the $TiO_2$ surface at a slower rate compared to common D-π-A organic dyes.

Under optimized test conditions for the lateral dyes **HY102** and **HY102-2**, the electrolyte without TBP was used. To explain the TBP effect on DSC performance, the electrolytes with 0.08 M TBP and without TBP for DSCs based on **HY102** were checked, and the performance of the solar cells are shown in Fig. 6. Upon the addition of TBP, although the $V_{oc}$ was improved, the $J_{sc}$ of the solar cell decreased significantly from 6.36 to 3.23 mA $cm^{-2}$ and thus $\eta$ dropped from 2.1% to 1.0%. It has been reported[12]

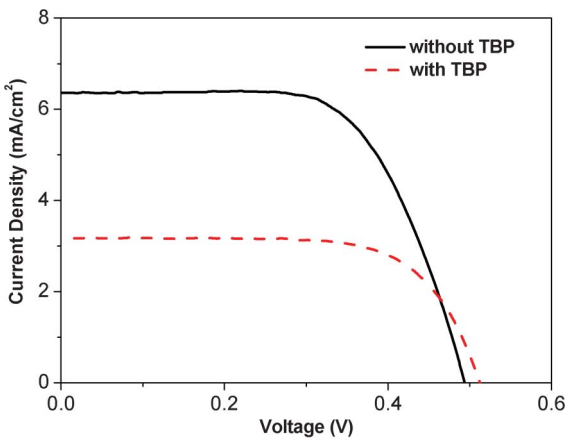


**Fig. 6** *J-V* curves of DSC based on **HY102** dye with electrolyte without TBP (0.6 M DMPII/0.2 M LiI/0.02 M $I_2$/0.1 M TBAI in AN:VN = 85:15) (solid line) and containing TBP(0.6 M DMPII/0.2 M LiI/0.02 M $I_2$/0.1 M TBAI/0.08 M TBP in AN:VN = 85:15) (dash line).

that TBP gives a significant improvement of the open-circuit potential of the solar cell. Several mechanisms have been proposed to explain the observed effects. Among of them, Nazeeruddin *et al.* showed that the dark current, due to reduction of triiodide by electrons in $TiO_2$, was suppressed by addition of TBP.[13] This was attributed to a blocking effect in virtue of the adsorption of TBP on the active sites at the $TiO_2$ surface. For our novel lateral dyes, the anchoring group and the electron injection group is separate. Firstly chemical bonding to $TiO_2$ surface by the anchoring group of lateral carboxylic acid took place, and then electrons are injected through the electron acceptor unit of cyano-groups close to the $TiO_2$ surface by proper spatial configurations. According to Nazeeruddin *et al.* the blocking effect due to adsorption of TBP on the $TiO_2$ surface would hinder the electron acceptor from coming into close contact with the $TiO_2$ surface, which would dramatically decrease the electron injection efficiency. As a result, the lowered $J_{sc}$ for dyes **HY102** and **HY102-2** with lateral anchoring group is attributed to the addition of TBP in electrolyte.

Fig. 7 shows the incident photon-to-current conversion efficiencies (IPCEs) data as a function of incident wavelength for DSCs based on three sensitizers. The IPCE spectra are consistent with the UV-vis absorption spectra on the $TiO_2$ film. The integral current densities calculated from IPCE spectra for three dyes all match well with *J-V* test results (Fig. 7). IPCE action spectrum for DSC based on **HY102** is broader than those of DSCs with **HY102-1** and **HY102-2**, from 400 nm to 800 nm. The maximum IPCE value for the three DSCs increased in the order of **HY102** < **HY102-2** < **HY102-1**. As shown in Table 1, there are just minor differences between LUMO levels for the three dyes, but big differences in maximum IPCE values observed, which mainly arise from the different electron injection efficiencies caused by the spatial configurations of these dyes after loading onto the $TiO_2$ surface, rather than the injection driving force. In other words, the electron injection efficiency follows the order of **HY102** < **HY102-2**< **HY102-1**, consistent with the order of the maximum IPCE values. The poor electron injection efficiency of **HY102** compared to **HY102-1** is mainly due to the non-ideal electron injection mode. The spatial electron transfer mode in **HY102** system is worse than electron injection through the chemical bond in **HY102-1** system. For the dye **HY102-2**, although there are two carboxylic acid groups, only the lateral one acts as the anchoring group. The other located at the end-group role to inject electron to the $TiO_2$ film is further from the $TiO_2$ surface, and so makes little contribution to the electron injection efficiency compared to **HY102**.

The different binding modes between $TiO_2$ surface and anchored dye are vital to achieve high quantum yields of electron injection into the semiconductor.[14] The carboxylate functional groups of dyes play a crucial role in interfacial binding between the dye and semiconductor. The resonance FTIR technique provides a direct demonstration on binding mode of dyes on $TiO_2$ surfaces. The FTIR spectra of our three dyes were measured as shown in Fig. 8. According to Deacon–Philips rule,[15] the binding modes of the dye on $TiO_2$ surface was determined by calculating the frequency separation, $\Delta V(V_{as}(COO^-)$ - $V_s(COO^-))$, between the asymmetric ($V_{as}$) and symmetric stretching ($V_s$) modes of the carboxylate unit. The $\Delta V$ values are in the order of unidentate > ionic form ≈

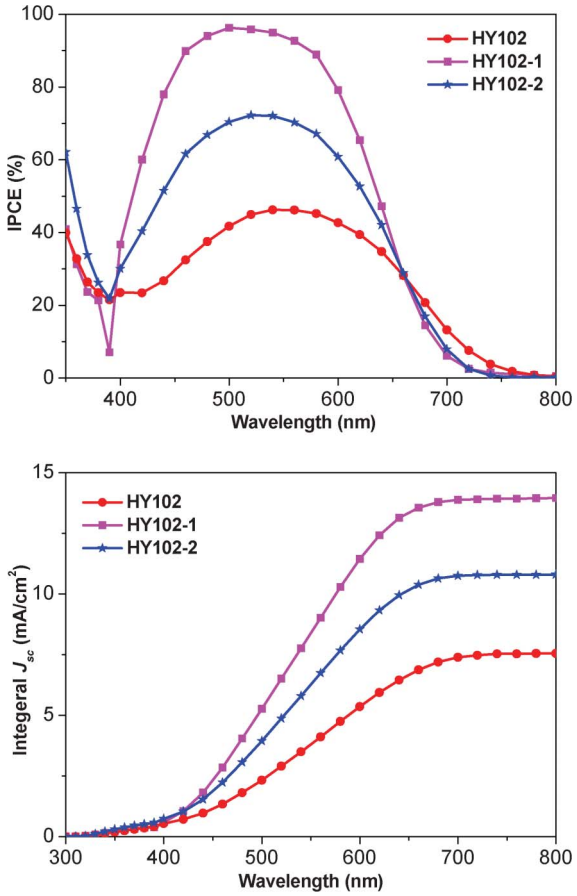


**Fig. 7** Spectral response of the photocurrent of DSC based on **HY102**, **HY102-1** and **HY102-2** dyes under optimized work conditions.

bidentate bridging > bidendate chelating. Yang *et al* has reported[14] that bidentate bridging is suggested for a majority of binding modes between semiconductor surface and anchored dye in $CH_2Cl_2$ solution. When the dyes anchored to $TiO_2$ surface in $CH_2Cl_2$, different $\Delta V$ values were obtained. The anchored three dyes **HY102**, **HY102-1** and **HY102-2** in $CH_2Cl_2$, showed different $\Delta V$ values of 231, 226, and 233 $cm^{-1}$, respectively. One can conclude therefore that the binding modes of these dyes on

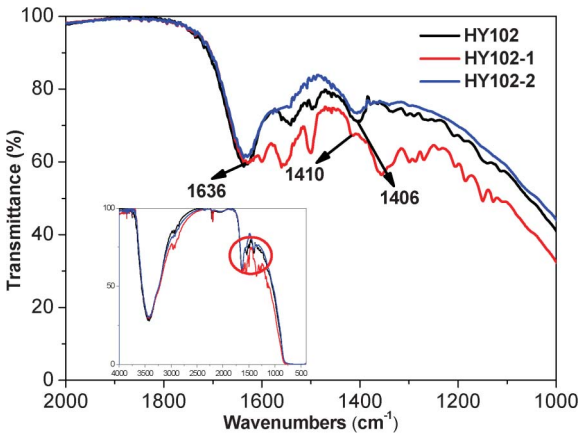


**Fig. 8** FTIR spectra of anchored **HY102**, **HY102-1** and **HY102-2** on $TiO_2$ *via* $CH_2Cl_2$.

the semiconductor surface should be the bidentate bridging configuration. The dyes **HY102** and **HY102-2** on $TiO_2$ film have similar resonance FTIR absorption spectra. It can be deduced that the dye **HY102-2** is supposed to anchor to $TiO_2$ surface by lateral flexible carboxylic acid group like **HY102**. However, the peak of carbonyl group was not observed at 1700–1750 $cm^{-1}$ for **HY102-2**. Considering the different $\Delta V$ value of **HY102-2** compared with that of **HY102-1**, the bonding between **HY102-2** and $TiO_2$ film by the single lateral flexible carboxylic acid group is absolutely predominant. The other carboxylic acid group contained in the cyanoacrylic acid unit is most probably deprotonated in the vicinity of $TiO_2$ surface, and injects electron to $TiO_2$ film by spatial transfer.

To understand the lower $V_{oc}$ for the DSCs based on **HY102** and **HY102-2** compared to those of DSC with the dye **HY102-1**, we carried out Electrochemical Impedance Spectroscopy (EIS) analysis[16] to study the interfacial charge transfer processes in DSCs. Fig. 9 shows the Nyquist plots for the DSCs with **HY102**, **HY102-1** and **HY102-2**. The large semicircle represents the charge recombination arising from electrons in the $TiO_2$ film recombination with $I_3^-$ ion in the electrolyte. Under the same experimental condition the charge transfer resistance at the $TiO_2$/dye/electrolyte interface increased from **HY102** to **HY102-2**, and **HY102-1** (Fig. 9). As previously mentioned, **HY102-1** showed a larger $V_{oc}$ compared to **HY102** and **HY102-2** due to addition of TBP in the electrolyte. Since the TBP on the $TiO_2$ surface acts as a blocking layer preventing the approach of $I_3^-$ ions to the $TiO_2$ surface, the recombination between the electrons in $TiO_2$ and the holes in electrolyte could be more dramatically suppressed for **HY102-1** than **HY102** and **HY102-2**. Moreover, the anchoring group of the lateral carboxylic acid on the donor part for dyes **HY102** and **HY102-2** brings the donor unit close to the $TiO_2$ surface, which is likely to induce electron recombination in the $TiO_2$ film with the oxidized dye. As a result, the combination of poor charge transfer and possible electron recombination with oxidized dye leads to a lower $V_{oc}$ for DSCs sensitized by **HY102** and **HY102-2** compared to **HY102-1**.

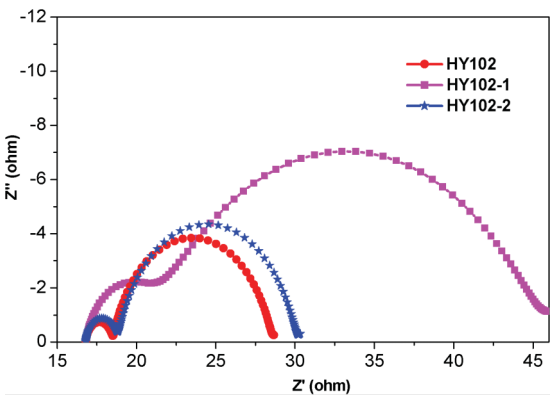


**Fig. 9** Electrochemical impedance spectra, scanned from $10^{-2}$ to $10^7$ Hz at room temperature, for the devices based on **HY102**, **HY102-1** and **HY102-2**, respectively: Nyquist plots; cells were measured at −0.7 V in the dark. The alternate current (AC) amplitude was set at 10 mV.

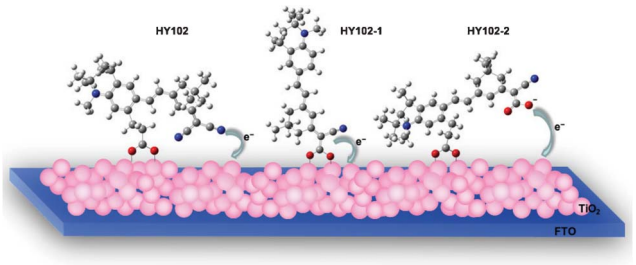


**Fig. 10** Schematic view of possible binding mode and electron injection for **HY102**, **HY102-1** and **HY102-2** on $TiO_2$ surface.

### Possible photo-induced electron transfer of three different types of D-π-A sensitizers

Fig. 10 shows an ideal electron injection diagram for DSCs based on nanocrystalline $TiO_2$ electrode, $I^-/I_3^-$ redox couple, and **HY102**, **HY102-1** and **HY102-2** as photosensitizers. **HY102-1** (contains a cyanoacrylic acid that incorporates an anchoring group and acceptor part as one) adsorbed on the $TiO_2$ surface and injected electron through carboxylic acid group with bidentate bridging mode. Unlike **HY102-1**, the lateral dye **HY102** bonded to the $TiO_2$ surface by bidentate bridging mode through the lateral flexible carboxylic acid group, but the electron was injected to $TiO_2$ through the electron acceptor unit of cyano groups close to the $TiO_2$ surface. **HY102-2** which contains both a lateral flexible carboxylic acid group and a cyanoacrylic acid group shows similar anchoring and electron injection behavior as **HY102**, as discussed above.

## Conclusions

In summary, we report one novel D-π-A organic dye **HY102** with a lateral anchoring group and two reference dyes **HY102-1** (containing cyanoacrylic acid group that combines electron acceptor and anchoring group together) and **HY102-2** (containing both cyanoacrylic acid group and lateral carboxylic acid group). Optimized test results indicate that the **HY102-1**-sensitized solar cell shows the best efficiency of 7.0% among all three dyes, which is attributed to highly efficient electron injection by cyanoacrylic acid unit and less charge recombination on the $TiO_2$ surface. The DSCs based on **HY102** and **HY102-2** exhibited decreased efficiencies of 3.6% and 2.7%, both lower $J_{sc}$ and $V_{oc}$ compared with **HY102-1**. This is attributed mainly to the anchoring mode by the lateral anchoring group, which causes the electron donor moiety close to the $TiO_2$ surface to enhance electron recombination, and makes the electron acceptor unit of cyanoacrylic acid move apart from the $TiO_2$ surface decreasing the electron injection efficiency.

## References

1 (*a*) M. Grätzel, *Nature.*, 2001, **414**, 338; (*b*) M. K. Nazeeruddin, P. Pechy, T. Renouard, S. M. Zakeeruddin, R. Humphry-Baker, P. Comte, P. Liska, L. Cevey, E. Costa, V. Shklover, L. Spiccia, G. B. Deacon, C. A. Bignozzi and M. Grtäzel, *J. Am. Chem. Soc.*, 2001, **123**, 1613; (*c*) M. K. Nazeeruddin, F. De Angelis, S. Fantacci, A. Selloni, G. Viscardi, P. Liska, S. Ito, B. Takeru and M. Grätzel, *J. Am. Chem. Soc.*, 2005, **127**, 16835; (*d*) Y. Chiba, A. Islam, Y. Watanabe, R. Komiya, N. Koide and L. Han, *Jpn. J. Appl. Phys.*, 2006, **45**, 638; (*e*) M. K. Nazeeruddin, T. Bessho, L. Cevey, S. Ito, C.

 

Klein, F. De Angelis, S. Fantacci, P. Comte, P. Liska, H. Imai and M. Grätzel, *J. Photochem. Photobiol. A.*, 2007, **185**, 331; (*f*) F. Gao, Y. Wang, J. Zhang, D. Shi, M. Wang, R. Humphry-Baker, P. Wang, S. M. Zakeeruddin and M. Grätzel, *Chem. Commun.*, 2008, **23**, 2635; (*g*) A. Hagfeldt, G. Boschloo, L. Sun, L. Kloo and H. Pettersson, *Chem. Rev.*, 2010, **110**, 6595–6663.

2 C. S. Karthikeyan, H. Wietasch and M. Thelakkat, *Adv. Mater.*, 2007, **19**, 1091–1095.

3 Y. Hao, X. Yang, J. Cong, H. Tian, A. Hagfeldt and L. Sun, *Chem. Commun.*, 2009, 4031–4033.

4 S. Yu, S. Ahmadi, M. Zuleta, H. Tian, K. Schulte, A. Pietzsch, F. Hennies, J. Weissenrieder, X. Yang and M. Göthelid, *J. Chem. Phys.*, 2010, **133**, 224704.

5 M. Ziółek, I. Tacchini, M. Teresa Martínez, X. Yang, L. Sun and A. Douhal, *Phys. Chem. Chem. Phys.*, 2011, **13**, 4032–4044.

6 (*a*) R. Chen, X. Yang, H. Tian, X. Wang, A. Hagfeldt and L. Sun, *Chem. Mater.*, 2007, **19**, 4007; (*b*) R. Chen, X. Yang, H. Tian and L. Sun, *J. Photochem. Photobiol. A*, 2007, **189**, 295.

7 K. H. Park, R. J. Twieg, R. Ravikiran, L. F. Rhodes, R. A. Shick, D. Yankelevich and A. Knoesen, *Macromolecules.*, 2004, **37**, 5163.

8 (*a*) A. Hagfeldt and M. Grätzel, *Chem. ReV.*, 1995, **95**, 49; (*b*) K. Kalyanasundaram and M. Grätzel, *Coord. Chem. Rev.*, 1998, **177**, 347.

9 D. P. Hagberg, T. Edvinsson, T. Marinado, G. Boschloo, A. Hagfeldt and L. Sun, *Chem. Commun.*, 2006, 2245–2247.

10 J. H. Yum, S. J. Moon, R. Humphry-Baker, P. Walter, T. Geiger, F. Nüesch, M. Grätzel and M. K. Nazeeruddin, *Nanotechnology.*, 2008, **19**, 424005.

11 H. Tian, X. Yang, J. Cong, R. Chen, C. Teng, J. Liu, Y. Hao, L. Wang and L. Sun, *Dyes Pigments.*, 2010, **84**, 62–68.

12 G. Boschloo, L. Häggman and A. Hagfeldt, *J. Phys. Chem. B.*, 2006, **110**, 26.

13 M. K. Nazeeruddin, A. Kay, I. Rodicio, R. Humphry-Baker, E. Müller, P. Liska, N. Vlachopoulos and M. Grätzel, *J. Am. Chem. Soc.*, 1993, **115**, 6382.

14 H. Tian, X. Yang, R. Chen, R. Zhang, A. Hagfeldt and L. Sun, *J. Phys. Chem. C.*, 2008, **112**, 11023–11033.

15 G. B. Deacon and R. Phillips, *J. Coord. Chem. Rev.*, 1980, **33**, 227–250.

16 (*a*) M. Adachi, M. Sakamoto, J. Jiu, Y. Ogata and S. Isoda, *J. Chem. Phys. B.*, 2006, **110**, 13872; (*b*) Q. Wang, J. Moser and M. Grätzel, *J. Chem. Phys. B.*, 2005, **109**, 14945; (*c*) Z. Wang, N. Koumura, Y. Cui, M. Takahashi, H. Sekiguchi, A. Mori, T. Kubo, A. Furube and K. Hara, *Chem. Mater.*, 2008, **20**, 3993; (*d*) D. Kuang, S. Uchida, R. Humphry-Baker, S. Zakeeruddin and M. Grätzel, *Angew. Chem., Int. Ed.*, 2008, **47**, 1923.